BNL-205744-2018-COPA

New Insights into Shape Memory Alloy Bimorph Actuators Formed by Electron Beam Evaporation

H. Sun, D. Nykypanchuk

Submitted to the ASME 2018 IDETC/CIE Conference
to be held at Quebec City, Canada
August 26 - 29, 2018

Center for Functional Nanomaterials
Brookhaven National Laboratory

U.S. Department of Energy
USDOE Office of Science (SC), Basic Energy Sciences (BES) (SC-22)

NEW INSIGHTS INTO SHAPE MEMORY ALLOY BIMORPH ACTUATORS FORMED BY ELECTRON BEAM EVAPORATION

Hao Sun
Northwestern Polytechnical University
710072 Xi'an, People's Republic of China

Jianjun Luo
Northwestern Polytechnical University
710072 Xi'an, People's Republic of China

Ming Lu
Brookhaven National Laboratory
Upton, NY, USA 11973

Dmytro Nykypanchuk
Brookhaven National Laboratory
Upton, NY, USA 11973

Yong Shi
Stevens Institute of Technology
Hoboken, NJ, USA 07030

ABSTRACT

In order to create shape memory alloy (SMA) bimorph microactuators with high-precision features, a novel fabrication process combined with electron beam (E-beam) evaporation, lift-off resist and isotropic XeF_2 dry etching method was developed. To examine the effect of E-beam deposition and annealing process on nitinol (NiTi) characteristics, the NiTi thin film samples with different deposition rate and overflow conditions during annealing process were investigated. With the characterizations using scanning electron microscope and x-ray diffraction, the results indicated that low E-beam deposition rate and argon employed annealing process could benefit the formation of NiTi crystalline structure. In addition, SMA bimorph microactuators with high-precision features as small as 5 microns were successfully fabricated. Furthermore, the thermomechanical performance was experimentally verified and compared with finite element analysis simulation results.

Key words: shape memory alloy, bimorph, electron beam evaporation, lift-off resist, XeF_2 dry etching, annealing, x-ray diffraction, microactuators, micro fabrication, NiTi

INTRODUCTION

Over the years, microactuators have already been widely applied in diverse applications, such as in aerospace (Kudva 2004), biomedical field (Petrini and Migliavacca 2011), and microrobotics (Song et al. 2016), which require delicate handling of micro-objects and high-precision coordination in limited microenvironment. Especially for three decades, the rapid advancements of microelectromechanical system (MEMS) technique has enabled the research of an extensive range of miniaturized microactuators using MEMS fabrication methods. Microactuators can be classified depended on the actuation principles into electrostatic (De Jong et al. 2010), piezoelectric (Liang et al. 2011), electromagnetic (Lin et al. 2014), thermal and shape memory alloy (SMA). SMA has such attractive advantages compared to other actuation mechanisms as high power density, large actuation force, large displacement range, low cost, resistance to corrosion, and biocompatibility (Barbarino et al. 2014), which make this kind of smart material one of the preferred microactuators in various specific applications, particularly in biomedical field (Nisar et al. 2008 and Erismis et al. 2010), such as endovascular surgery, neural interfaces, drug delivery and intestinal obstruction. Among various SMA materials, a nickel titanium (NiTi) SMA composition is commonly used.

However, SMA actuators have also been often described as having a slow response speed, which is seen as a major hindrance for the broad implementation (Loh et al. 2006). The main limiting reason for its slow response speed is the heating and cooling speed of the SMA (Velazquez and Pissaloux 2012). To overcome this drawback, NiTi thin film SMA in MEMS has been studied since 1990, when it was presented by Walker (1990), not only because the NiTi thin film can provide larger forces over longer displacements, but also since the challenges of slow response speed can be overcome significantly by NiTi thin film due to the larger surface area to volume ratio. As a result, the advancements of microactuators formed by NiTi thin film have further achieved with various applications, which have been developed in MEMS field. For example, Takeuchi and Shimoyama (2000) as well as Fu et al. (2008) fanricated a microgripper, Makino et al. (2010) as well as Sassa et al. (2012) presented a micropump, and Chung and Chan (2011) fabricated a micro imaging sensor. To date, the NiTi thin film has been fabricated by several deposition techniques, namely, radio frequency (RF) or direct current (DC) magnetron sputtering,

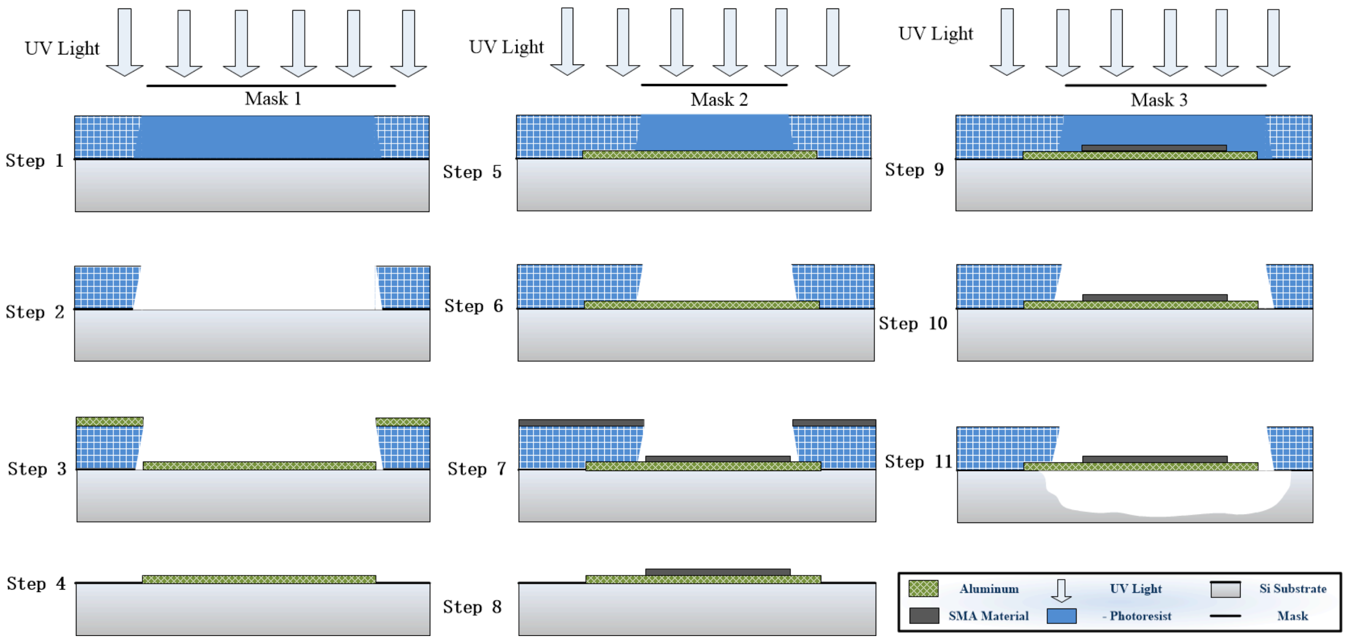

Figure 1. Fabrication process using E-beam evaporation

pulse laser deposition, plasma enhanced chemical vapor deposition, and flash evaporation (Mohammad et al. 2015). The most common deposition method is sputtering. In the paper (Wongweerayoot et al. 2014), a bimorph microgripper was fabricated by depositing NiTi thin film on a freestanding copper using DC sputtering. According to this research, the microgripper could grasp and hold a plastic ball up to 0.5 mg weight. However, this NiTi thin film deposition technique poses a challenge in term of controlling element composition resulting from deviation in sputtering yields from original target material (Hae et al, 2000). During the deposition process, parameters such as temperature, pressure, post-annealing conditions, power applied and so on should be precisely controlled to obtain the expected stoichiometry, which has a large effect on the transformation temperature. To obtain better uniformity of NiTi composition, Hae (2000) used electron beam evaporation method to fabricate NiTi thin film instead of the sputtering, which can be explained by the elimination of oxidation loss by employing high power to result in a shorter evaporation time, as well as better vacuum conditions. However, microstructure formed by NiTi thin film was not particularly studied in this paper. On the other hand, very uniform micro-patterns of NiTi thin film are required in many specific applications (Chun et al. 2009). Based on the sputtering deposition method, one common fabrication process of NiTi thin film micro-patterns is wet etching, which utilizes a dilute solution of hydrofluoric acids, nitric acids, and DI water (Fu et al. 2004). But this kind of fabrication process produces non-uniform micro-patterns with severe undercuts. To achieve micropatterns with smooth edges, an anisotropic dry etching method has been proposed (Zamponi et al. 2008). But a large drawback of this method is the slow etching rate, which is unacceptable in many cases. As a result, until now, it has been difficult to micromachine NiTi thin film with high-precision features as small as 5 microns, which is quite meaningful in extremely microenvironment applications. Hence, there is a huge demand to develop a new approach to fabricate SMA microactuators formed by NiTi thin film with small features to meet specific requirements in various fields.

In this paper, SMA bimorph microactuators with NiTi thin film and aluminum (Al) have been developed using a novel fabrication process. This kind of SMA microactuators with high-precision features as small as 0.5um were fabricated by combining with electron beam evaporation, lift-off resist and isotropic XeF_2 dry etching method. This paper demonstrated the feasibility to fabricate NiTi SMA microstructure using E-beam deposition method and analyzed characterizations of NiTi SMA material when the conditions of deposition and annealing process were varied. The effect of the conditions mentioned above on the characterizations, which were performed using isotropic XeF_2 dry etching machine, scanning electron microscope (SEM), and x-ray diffraction (XRD), were highlighted. Moreover, the simulation results of thermomechanical behavior of SMA bimorph microactuators were studied, which utilized the finite element analysis method via Coventor Ware. In addition, the thermomechanical performance of the SMA bimorph microactuator was experimentally verified and compared with simulation results.

FABRICATION PROCESS

In this paper, a novel fabrication processes for producing SMA microactuators with high-precision features were presented. For every fabrication step, the approach used to construct the features was described.

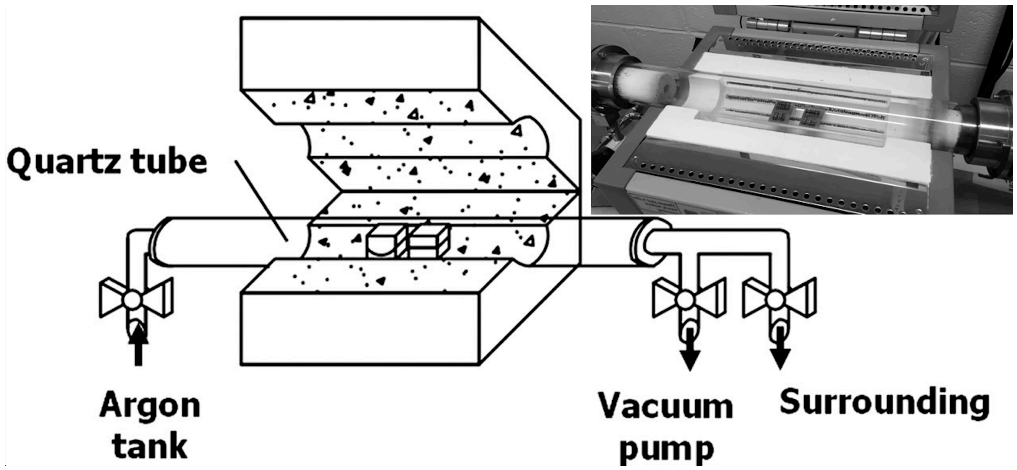

Figure 2. Schematic setup of quartz tube furnace with argon overflow

Figure 1 separately illustrates the lift-off resist process, electron beam evaporation process and isotropic dry etching process utilized to fabricate SMA microactuators with high-precision patterns. It started by initially depositing aluminum thin film with 500 nm thickness by the photolithography and E-beam technique. Beginning with a 4-inch P-type silicon wafer, spinning coating of negative photoresist MaN1410 for UV exposure (step 1, 3000rpm for 30s with 1um thickness and $10mW/cm^2$ UV light for 40s with Mask 1) was performed, which was followed by development (step 2, Mad 533/S, 60s). The removal parts of negative photoresist formed the desired patterns with high-precision could be up to 0.5 microns. Then 500 nm aluminum thin film was deposited on the surface of silicon wafer by E-beam evaporation on a high vacuum condition (step 3, base pressure below 10^{-6} Torr). After achieving the desired thickness, the rest of negative photoresist with aluminum deposited on the surface of photoresist were lifted-off using strong organic solvent 1165 (step 4, 60 minutes at 80 Celsius) to form patterned aluminum thin film thanks to the perfect directivity of E-beam deposition technique. Consequently, a patterned NiTi thin film with 500 nm thickness was deposited on the aluminum thin film layer by the similar fabrication technique to achieve bimorph structure and the minimum feature size involved was about 5 microns. (step5, step 6, step 7 and step 8). Following the aluminum and NiTi thin film E-beam deposition, a MaN1410 negative photoresist was spun coated and patterned via similar photolithography technique on the surface of silicon wafer (step 9 and step 10, 1000rpm for 30s with 2um thickness, $10mW/cm^2$ UV light for 60s with Mask 3 and develop in Mad 533/S for 80s) and the exposed silicon material was etched using XeF_2 by isotropic dry etching technique to release bimorph microstructures (step 11, etching rate is approximately 60 s to etch 0.5 microns thickness of silicon material). Finally, one end fixed SMA bimorph microactuators were crystallized in a quartz tube furnace at the desired annealing temperature 600°C to perform the annealing process.

EXPERIMENTAL SETUP

Since the research result about NiTi thin film deposited by E-beam technique has little, there is no systematic study of E-beam deposited NiTi microactuators, relevant literatures are rare. Hence, the effects of the E-beam deposition process and annealing conditions were firstly investigated with various E-beam deposition powers and different vapor flow conditions as shown in Table 1.

Table 1 Samples under different deposition and annealing process

Sample	Deposition Rate (nm/s)	E-beam Current (mA)	Annealing Process	Overflow
1	0.06	167	No	
2	0.06	167	Yes	Vacuum
3	0.06	167	Yes	Argon
4	0.15	196	No	
5	0.15	196	Yes	Vacuum
6	0.15	196	Yes	Argon

In this work, the preparation of NiTi thin film was done on standard P-type silicon wafer by the E-beam evaporation, as this kind of wafer could not only be isotropically etched by the XeF_2 etcher, but also was thermally stable during alloy characterization. The NiTi thin film was deposited by electron beam evaporation (Lesker PVD75) using a NiTi alloy material with ratio of Ti and Ni equaled to one. During the E-beam deposition process, the base pressure was set at 10^{-6} Torr and the accelerating voltages was maintained at 7.8 kV. At these conditions, the deposition rate of NiTi thin film can be controlled using different beam current and DC power. Afterwards, the NiTi thin film samples were separately annealed at different vapor overflow conditions in the quartz tube furnace, as shown in Fig. 2., to crystallize NiTi alloy. At first, vacuum pump was used to remove the air inside the quartz tube. Then the vacuum pump was turned off, and argon was employed to make oxygen free in the quartz tube. To avoid oxidation of NiTi thin film, this procedure was repeated three

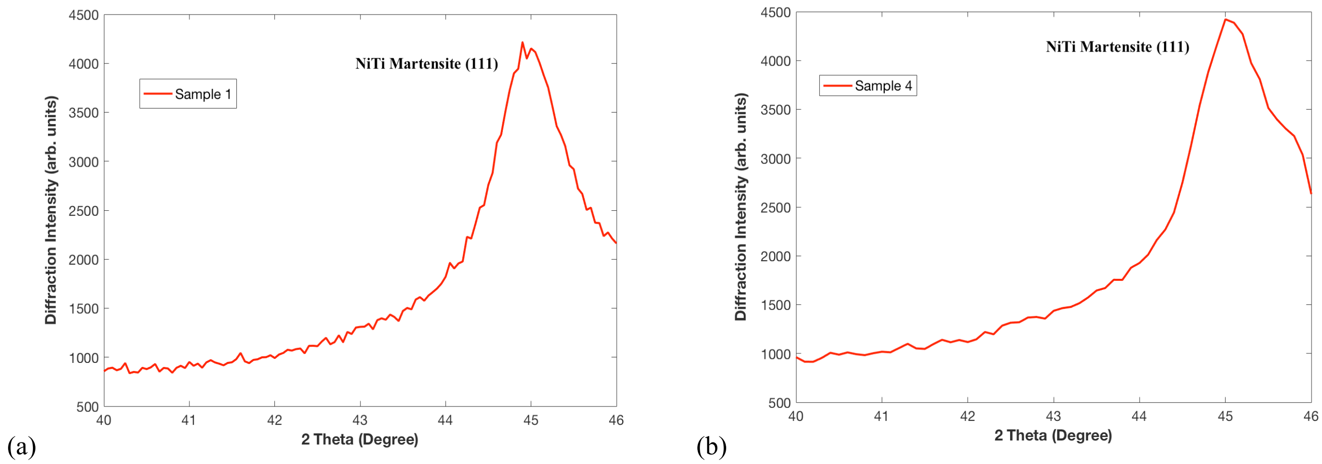

Figure 3. XRD results of NiTi thin film under different deposition rate

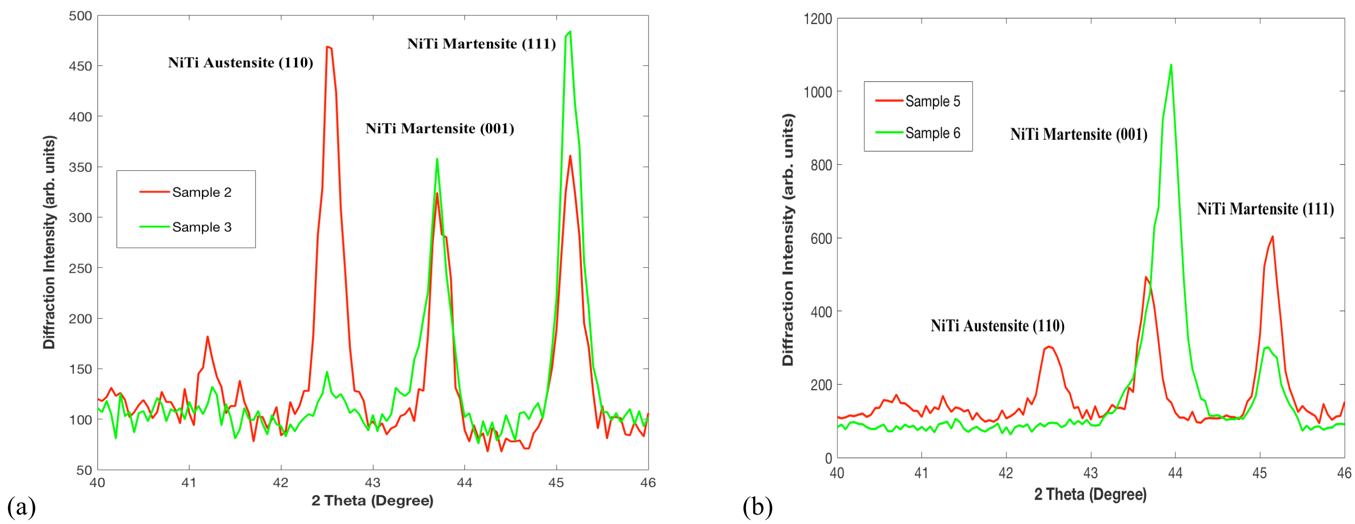

Figure 4. XRD results of NiTi thin film with different overflow conditions during annealing process

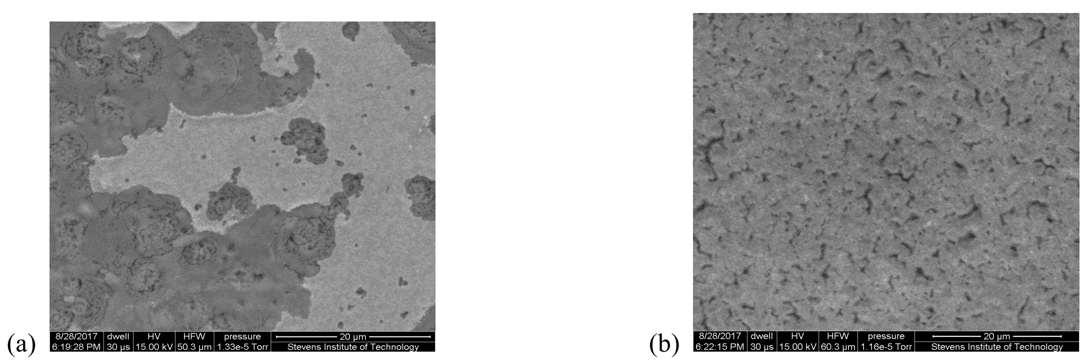

Figure 5. SEM images of surface of annealed NiTi thin film fabricated under low E-beam deposition rate: (a) image of sample 2 with argon overflow during annealing, (b) image of sample 3 without argon overflow during annealing

times. At last, the heater was turned on with a heating rate of 600°C/ hr. Once reached the desired annealing temperature 600°C, the temperature was kept constant for 1 hour, and then, the heater was turned off to obtain a natural cooling procedure.

To study crystallinity of NiTi thin films, x-ray diffraction spectra of these samples were measured using x-ray diffractometer (Rigaku Ultima III). In addition, SEM images (Hitachi S-4800) were utilized to analyze the surface of NiTi thin film as well as to evaluate the high-precision patterned NiTi microactuators.

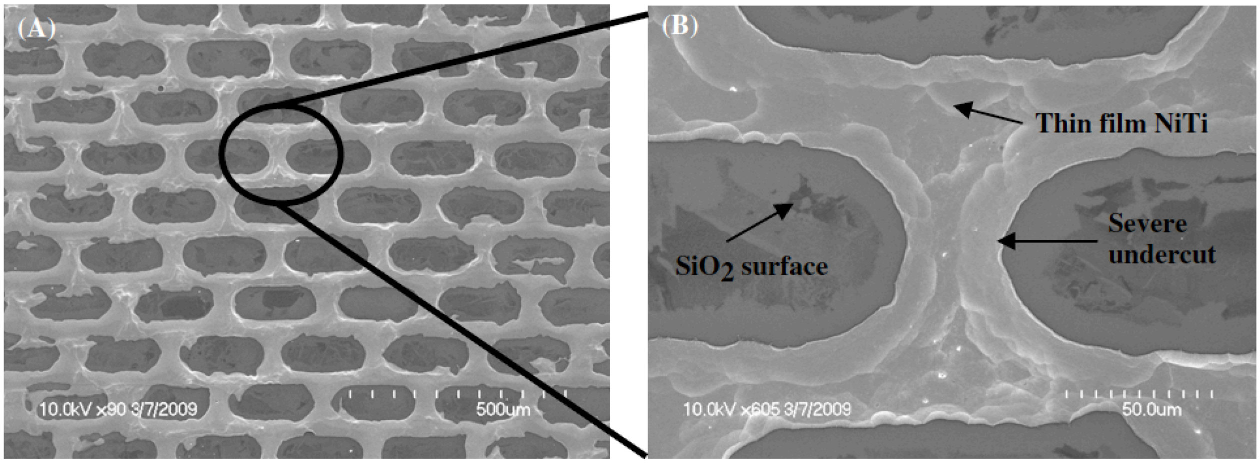

Figure 6. SEM images of wet etching process: (a) non-uniform patterns and (b) severe undercuts

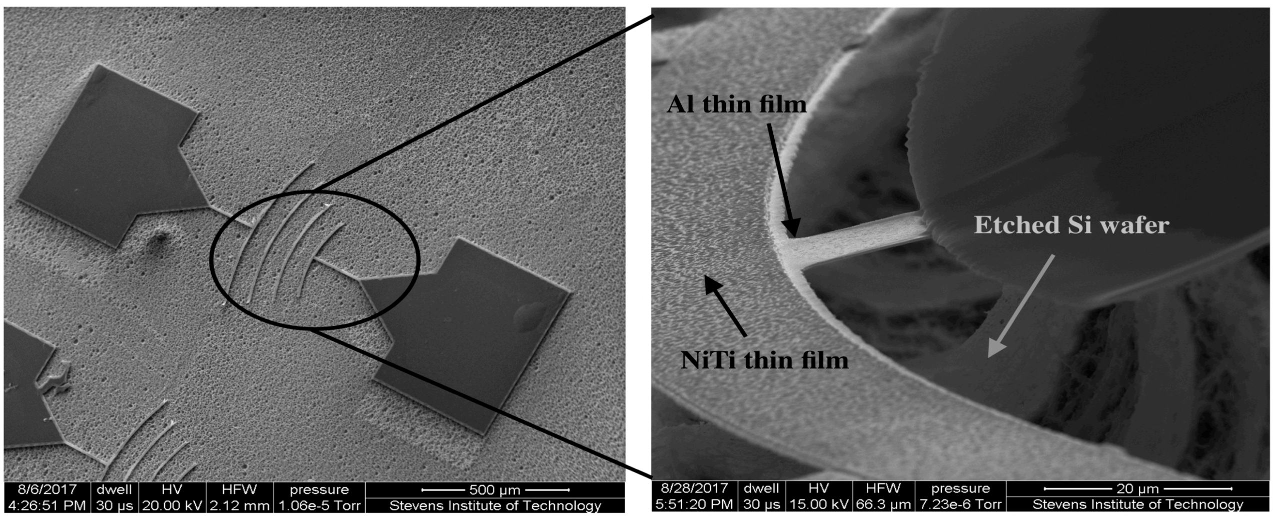

Figure 7. SEM image of patterned NiTi-Al bimorph microactuators with high-precision features as small as 10 microns using the novel fabrication method proposed in this paper

RESULTS AND DISCUSSION

Material characterization

In this study, the effect of E-beam deposition rate and annealing parameters on the material characterization was investigated. As shown in Table 1, the crystalline structures of six types of NiTi thin film samples were determined by XRD tests at room temperature. Figure 3(a) and (b), respectively, illustrated XRD test results of sample 1 and sample 4 with different E-beam deposition rate. In these two samples, it was obvious that the results exhibit only one similar peak (2theta=45°), which was identified as NiTi monoclinic structure (111) (martensite B19'). Subsequently, according to Fig. 4(a) and (b), with the same overflow annealing conditions, the XRD results showed the similar XRD patterns with different deposition rate. Seemingly, the deposition rates under different E-beam work power had little effect on the crystallization of NiTi thin film. However, it was found that the annealing overflow conditions showed great influence on the XRD results. For sample 2 and 5, totally three strong peaks can be found, one peak (2theta=42.5 °) corresponded NiTi cubic structure (110) (austenite B2), and the other two peaks (2theta=43.7°and 45°) were identified as (111) and (001) NiTi monoclinic structure (martensite B19'), which revealed that austenite and martensite co-exist in the same annealed NiTi thin films at room temperature and the phase transformation was confirmed. But for those two samples 3 and 6 without employing argon overflow during the annealing process, XRD test results only exhibited two strong peaks, and did not show any peak stand for austenite phase of NiTi. The XRD results indicate that the crystalline structure of NiTi thin film became better oriented when employed argon overflow during annealing process. In addition, it was also observed that the dominant phase was austenite in Figure 4 (a) of sample 2, which means the annealed NiTi thin film with low deposition rate could have better shape memory effect.

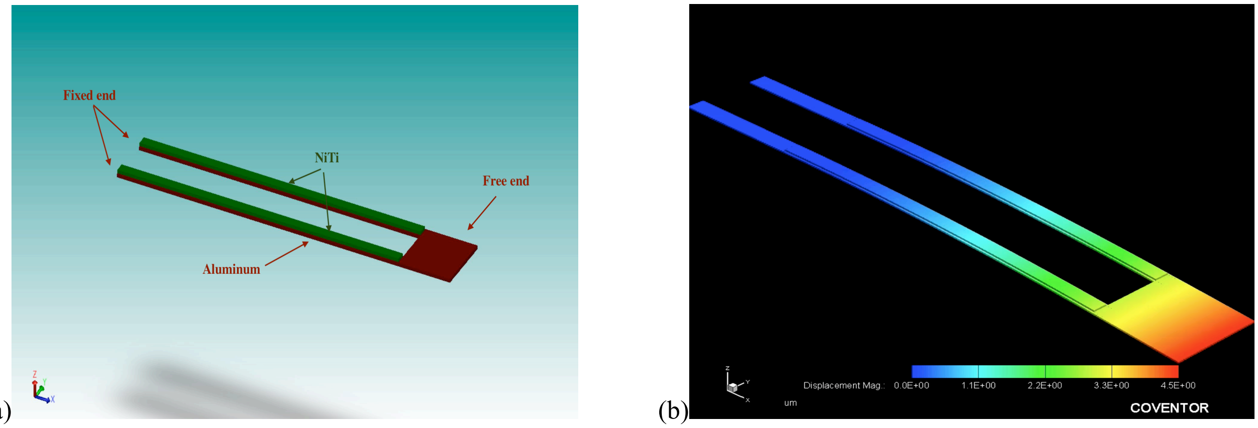

Figure 8. Thermomechanical behaviors of SMA bimorph microactuators investigated using the finite element analysis method via Coventor Ware: (a) SMA bimorph microactuators model, (b) thermomechanical simulation result

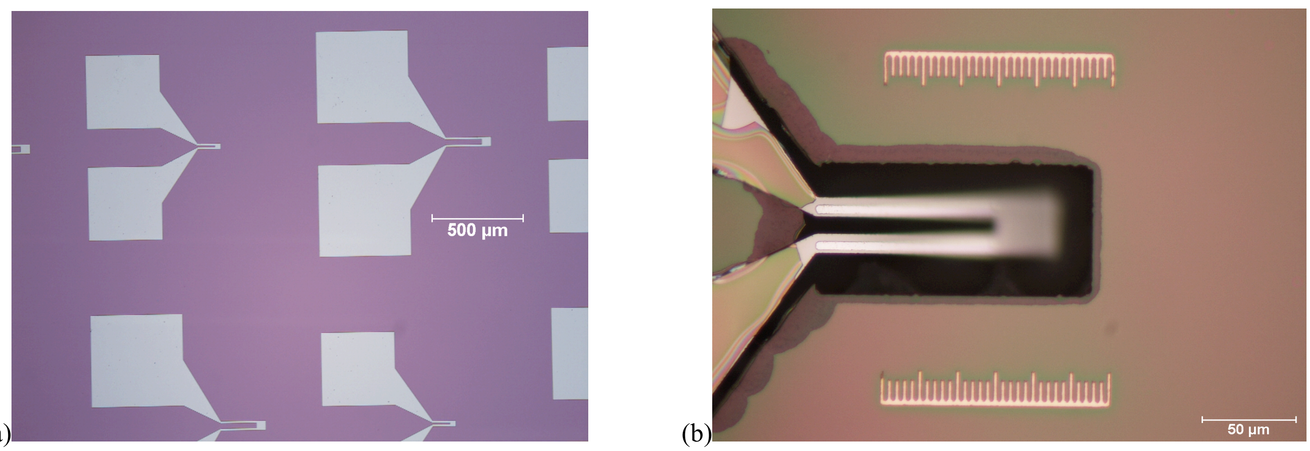

Figure 9. Optical microscope images of bimorph SMA microactuators before and after dry etching process: (a) before dry etching process, (b) after dry etching process.

Figure 5 (a) and (b) showed SEM images of surface of annealed NiTi thin film fabricated under low E-beam deposition rate. For sample 2 with argon overflow during annealing, the surface appeared brightly or shiny as shown in Fig. 5(a). In contrast, for sample 3 without employing argon overflow, the surface was cloudy or dark as shown in Fig. 5(b). This was because the crystalline austenite NiTi thin film of sample 2 were formed, compared to sample 3 without the crystalline austenite phase NiTi thin film oriented, which agreed with XRD results of Fig. 4 (a).

Fabricated Patterns

Figure 6 showed SEM images of patterned NiTi microstructure fabricated utilizing the standard wet etching method (Chun et al. 2010). Various types of geometries (i.e., triangles, circles) were fabricated with this etch approach and Fig. 6 was a representative sample. According to Fig. 6, even though the sizes of micropattern features were already 50 microns, it was obvious to find the presence of non-uniform patterns with severe undercuts. The challenge of this wet etching method shown are attributed to the isotropic etching mechanism present in NiTi thin film using a dilute solution of hydrofluoric acids, nitric acids, and DI water. When the etched patterned microstructures were released from the silicon wafer, it could be obviously found that the serious tearing problems existed near the undercuts.

In contrast, Fig. 7 showed an SEM image of patterned NiTi-Al bimorph microactuators with high-precision features as small as 10 microns, which were fabricated using the novel fabrication method proposed in this paper. Both the low magnification and high magnification SEM images were taken after releasing SMA microstructures from the silicon wafer using XeF_2 dry etcher. In addition, Fig. 8(b) illustrated that even in the features with sharp corners, this novel fabrication method produced quite smooth micropatterns relatively robustly. Furthermore, thanks to the perfect unique reactivity with silicon material using XeF_2, these NiTi micropatterns did not induce the fracture or tearing problems mentioned above after releasing from silicon wafer. Since this fabrication process combined with lift-off resist (LOR) process, electron beam evaporation (E-beam) process and isotropic dry etching process, as a result, the limit of fabrication precision was attributed to the limits of photolithography, which depended on the UV wavelength utilized during the exposure process.

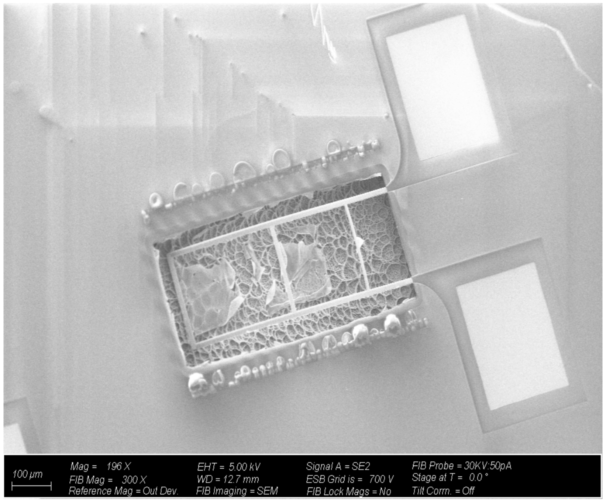

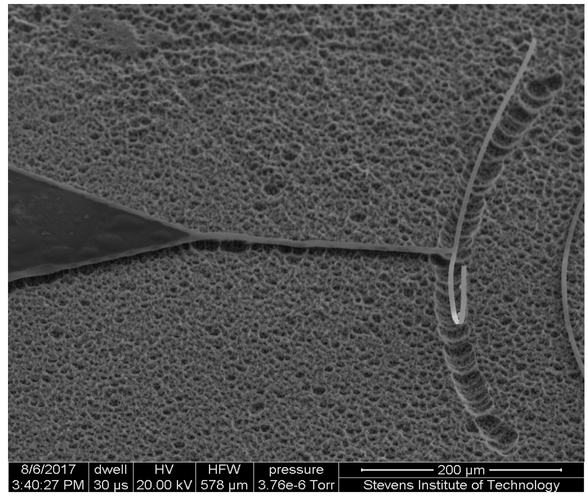

Figure 10. SEM pictures of other types of bimorph SMA microactuators in the static response experiments

SMA Bimorph Microactuator

Following successful E-beam depostion of patterned NiTi thin film, aluminum was chosen as the stress layer for the fabrication of micro NiTi-Al bimorph actuators. With combination of NiTi and aluminum, these bimorph microactuators could bend due to the mismatch in coefficient of thermal extension (CTE) between two different materials when structure temperature changed.

Table 2 Thermomechanical Properties of NiTi and Al

Properties	NiTi	Al
CTE (10^{-6} 1/K)	6.6 (Martensite) 11 (Austenite)	23.1
Density (g/cm^3)	6.45	2.7
Young's modulus (G Pa)	80	70
Poisson's ratio	0.3	0.35

Firstly, the thermomechanical behaviors of SMA bimorph microactuators were investigated using the finite element analysis method via Coventor Ware. As shown in Fig. 8(a), the SMA bimorph microactuators finite element model was built, with one end fixed and on end free. The red parts stranded for the main body of microactuators using aluminum material, and the green part employed as stress layer using NiTi thin film to induce residual stress throughout whole structure to make this bimorph microactuators bend. To determine the displacement of the bimorph SMA microactuator, FEA simulations were performed using the thermomechanical properties as shown in Table 2. As a result, Fig. 8(b) showed the maximum displacement (4.43 microns) of the microactuator, which was consisted of a 0.5 microns layer of NiTi deposited on the surface of 0.5 microns layer of aluminum at 200 °C.

Figure 9 (a) and (b), respectively, showed the bimorph SMA microactuators before and after dry etching process observed by optical microscope. The microactuators had two legs, 10×200 micron, connected together with a 50×50 micron square pad at a free end and two fixed contact pads at the other. Before releasing from silicon wafer as shown in Fig. 9 (a), the whole microstructures were fixed. Following XeF_2 etching process, the SMA bimorph microactuators were released from silicon as shown in Fig. 9 (b), and significant bending result could be observed. With the help of "ruler" deposited next to the microactuators, the maximum displacement (4.37 um) could be calculated using the equation of the radius of curvature in bent microactuators (Alaa et al. 2015), which was experimentally verified compared with FEA simulation results.

Furthermore, Fig. 10 (a) and (b) showed the SEM pictures of other types of bimorph SMA microactuators in the static response experiments, which demonstrated the feasibility to fabricate NiTi SMA microstructure using the novel deposition method proposed in this paper.

CONCLUSION

The standard wet etching method used to fabricate sputtering NiTi microstructure produced non-uniform micro-patterns with severe undercuts. In this paper, to solve the above problems, a novel fabrication method combined with electron beam evaporation, lift-off resist and isotropic XeF2 dry etching method was evaluated, which could fabricate SMA microactuators with high-precision features as small as 5 microns. In addition, the effects of E-beam deposition rate and annealing overflow conditions on the material characteristics were examined. The following conclusion could be drawn. The low E-beam deposition rate and argon employed annealing process would benefit the formation of the crystalline structure of the NiTi thin film. At the end, the SMA bimorph microactuators were successfully fabricated, and the thermomechanical performance was experimentally verified and compared with FEA simulation results. This work may contribute to a cost-effective fabrication process for versatile thrombus retrieving devices, which could also show promising application for micro-robotics.

ACKNOWLEDGMENTS

The authors most gratefully appreciate funding provided for this work by the Stevens NPU Ph.D. program from China Scholarship Council. Also, this research used resources of the Center for Functional Nanomaterials, which is a U.S. DOE Office of Science Facility, at Brookhaven National Laboratory under Contract No. DE-SC0012704.

REFERENCES

Alaa A. Z., Marwan N., Ahmad A. M. F., Suhail K., Mohamed S. M. A., 2015, "Thermomechanical behavior of bulk NiTi shape-memory-alloy microactuators based on bimorph actuation," *Microsyst Technol*, Vol. 7, pp. 132-141.

Barbarino, S., Flores, E. S., Ajaj, R., Dayyani, I. and Friswell, M., 2014, "A review on shape memory alloys with applications to morphing aircraft," *Smart Mater. Struct.* Vol.23, pp. 63-71.

Chun Y. J., Levi D. S., Mohanchandra K. P., Vinuela F. and Carman G. P., 2009, "Manufacturing and in vivo testing of thin film NiTi micro-engraft," *J. Am. Soc. Artif. Intern. Organs,* Vol. 55, pp. 167-181.

C.Y. Chung and P.M. Chan, 2011, "NiTi Shape Memory Alloy Thin Film Micro-Cantilevers Array," *Thin Solid Films*, Vol. 519, pp. 5307–5309.

De Jong B.R., Brouwer D.M., et al., 2010, "Design and fabrication of a planar three-DOFs MEMS-based manipulator," *Microelectromech Syst*, Vol.19(5), pp. 1116–30.

Erismis M.A., Neves H.P., et al., 2010, "A water-tight packaging of MEMS electrostatic actuators for biomedical applications," *Microsyst Technol,* Vol. 16, pp. 2109–2113

E. Makino, T. Mitsuya, and T. Shibata, 2001, "Fabrication of TiNi Shape Memory Micropump," *Sens. Actuators A*, Vol. 88, pp. 256–262.

Fu Y., Du H., Huang W., Ahang S. and Hu M., 2004, "TiNi-based thin films in MEMS applications: a review," *Sensors Actuators* Vol. 112, pp. 395–408.

F. Sassa, Y. Al-Zain, T. Ginoza, S. Miyazaki, and H. Suzuki, 2012, "Miniaturized Shape Memory Alloy Pumps for Stepping Microfluidic Transport," *Sens. Actuators B*, Vol. 165, pp. 157–163

Hae Y. N., Kyu H. L., Xiang X. C. and Chong S. C., 2000, "The Composition and Structure of NiTi Thin Film Formed by Electron Beam Evaporation," *Scripta material*, Vol. 43, pp. 847-852.

Kudva, J.N., 2004, "Overview of the DARPA Smart Wing Project," *Intell. Mater. Syst. Struct.*, Vol.15, pp. 261–267.

Liang Q., Zhang D., et al., 2011, "Six-DOF micro-manipulator based on compliant parallel mechanism with integrated force sensor," *Robot Com Int Manuf*, Vol. 27, pp. 124–34.

Lin S., Chang S., Li B., 2014, "Gearshift control system development for direct-drive automated manual transmission based on a novel electromagnetic actuator." *Mechatronics* Vol. 24, pp. 1214–22.

Loh, C. S., Yokoi, H. and Arai, T., 2006, "Natural heat-sinking control method for high-speed actuation of the SMA," *Int. J. Adv. Robot. Syst,* Vol.3, pp.213-221

Mohammad A. Z., Shafishuhaza S. and Mohamed S. M. A., 2015, "Micromachined Shape-Memory-Alloy Microactuators and Their Application in Biomedical Devices", *Micromachines*, Vol. 6, pp. 879-901.

Nisar A., Afzulpurkar N., Mahaisavariya B., Tuantranont A., 2008, "MEMS-based micropumps in drug delivery and biomedical applications," *Sens Actuators*, Vol.130, pp. 917–942

Petrini, L., Migliavacca, F. 2011, "Biomedical Applications of Shape Memory Alloys," *J. Metall.*, pp. 1–15.

Sung, H.S., Jang, Y.L., et al., 2016, "35 Hz SMA actuator with bending-twisting mode," *Scientific Reports*, pp. 1-13

S. Takeuchi and I. Shimoyama, 2000, "A Three-Dimensional Shape Memory Alloy Microelectrode with Clipping Structure for Insect Neural Recording," *Microelectromechanical Syst.*, Vol. 9, pp. 24–31.

Velazquez, R. and Pissaloux, E. E., 2012, "Modelling and Temperature Control of Shape Memory Alloys with Fast Electrical Heating," *Int. J. of Mechanics and Control*, Vol.13.

Walker, J.A., Gabriel, K.J., Mehregany, M., 1990, "Thin-film processing of TiNi shape memory alloy," *Sens. Actuators A Phys*., Vol.21, PP. 243–246.

Wongweerayoot, E., Srituravanich, W., Pimpin, A, 2014, "Fabrication and Characterization of Nitinol-Copper Shape Memory Alloy Bimorph Actuators," *J. Mater. Eng. Perform.* Vol. 24, pp.635–643.

Y. J. Chun, D. S. Levi, K. P. Mohanchandra1, M. C. Fishbein and G. P. Carman, 2010, "Novel micro-patterning processes for thin film NiTi vascular devices," Smart Materials and Structures, Vol. 19, pp. 21-30.

Y. Q. Fu, J.K. Luo, S.E. Ong, S. Zhang, A.J. Flewitt, and W.I. Milne, 2008, "A Shape Memory Microcage of TiNi/DLC Films for Biological Applications," *Micromech. Microeng.*, Vol. 18, pp. 035026.

Zamponi C., Rumpf H., Schmutz C. and Quandt E., 2008, "Structuring of sputtered superelastic NiTi thin films by photolithography and etching," *Mater. Sci. Eng. A* Vol.481, pp. 623–5.